Twenty-Third Symposium (International) on Combustion/The Combustion Institute, 1990/pp. 107–114

EXPERIMENTAL AND THEORETICAL STUDY OF THE RECOMBINATION REACTION $CH_3 + CH_3 \rightarrow C_2H_6$

DIETER WALTER AND HORST-HENNING GROTHEER
DLR, Institute for Physical Chemistry of Combustion
Pfaffenwaldring 38, D-7000 Stuttgart 80, West Germany

JOANNE W. DAVIES AND MICHAEL J. PILLING
Physical Chemistry Laboratory, South Parks Road, Oxford, OX1 3QZ, United Kingdom

AND

ALBERT F. WAGNER
Chemistry Division, Argonne National Laboratory, Argonne, IL 60439, USA

New measurements at 200 K, 300 K and 408 K are reported for the rate constant for the self-recombination of methyl radicals in Ar buffer gas. The 200 K measurements were made using laser flash photolysis while the 300 K and 408 K measurements were carried out at low pressures in a flow reactor. A variational RRKM calculation was performed to represent these new measurements and those previously published. The comparison between theory and experiment supports both a negative temperature dependence to the high pressure limit of recombination and a substantial positive temperature dependence to $\langle \Delta E \rangle_{tot}$, the average energy transferred in an Ar-C_2H_6* collision. An analytic representation of the recombination rate constant valid for all pressures where the rate constant exceeds 10^{-12} cm^3/molecule-sec is determined over the temperature range of 200 K to 2000 K.

Introduction

A recombination reaction of considerable importance in hydrocarbon combustion is

$$CH_3 + CH_3 \rightleftharpoons C_2H_6^* \xrightarrow{M} C_2H_6 \qquad (1)$$

where C_2H_6* is the initially formed metastable ethane and M is a stabilizing third body buffer gas. This reaction is a major termination step in pyrolysis and oxidation[1] and is a frequent reference reaction in kinetic studies of radical-molecule reactions.[2] Because of this, it has received considerable experimental attention over a large range of temperature and pressure.[2–8] The majority of the earlier studies[2–4] were indirect. The most recent studies[5–8] have been direct and extensive with over 130 measurements in the temperature range from 300 K to 900 K and pressures ranging from a few torr to several hundreds of torr of Ar.

Reaction (1) has also received considerable theoretical attention.[5,9–15] This theoretical interest is not only a response to the experimental work but also a manifestation of the proto-typic nature of Rxn. (1) as a barrierless reaction with many loose, anharmonic degrees of freedom. Several theoretical studies[5,9,15] did not treat the barrierless reaction path in fully rigorous way (by inclusion of variational effects, i.e., entropic, as well as energetic constraints, in locating the transition state that is the controlling bottleneck to reaction). However in most later studies,[10–14] this was an important aspect of the calculation. Three of these studies[12–13,15] have achieved, with different dynamical theories and parameterized potential energy surfaces, comprehensive agreement with the available direct measurements. Two of these studies[12,15] have produced an analytic functional form suitable for kinetics modelling studies that represents the calculated rate constants over a broader range of temperatures and pressures than that surveyed by the recent measurements.

As extensive as the experimental-theoretical record is on Rxn. (1), there are still important issues regarding the kinetics of this rection that can be addressed only by additional work. Two of relevance to this paper are: (1) what is the temperature dependence of the stabilization rate constant and

(2) what is the temperature dependence of the high pressure limit.

The first issue can be framed in a precise, if approximate, manner. The pressure dependence (i.e., the [M] dependence) of Rxn. (1) has been primarily represented by an effective stabilization rate constant k_s of a form first developed by Troe.[16]

$$k_s = \beta(\langle\Delta E\rangle_{tot}) \times k_{gas\text{-}kinetic} \qquad (2)$$

where $k_{gas\text{-}kinetic}$ is the gas kinetic rate constant for the collision of M with C_2H_6* and β is the probability that such a collision leads to stabilization of C_2H_6*. The major uncertainty in determining k_s is the value of β. Under a variety of circumstances,[16,17] β can be shown to be largely dependent on only one unknown, the average total energy transfer $\langle\Delta E\rangle_{tot}$ between the metastable addition complex and the buffer gas. The issue to be addressed is what, if any, is the temperature dependence of $\langle\Delta E\rangle_{tot}$?

This question can not be answered with the current experimental information according to Ref. 12 where a parameterized form of $\langle\Delta E\rangle_{tot}$ was adjusted in a theoretical calculation to reproduce the measured rate constants. It was found that for most of the 600 K temperature range surveyed experimentally, the rate constants measured were too close to the high pressure limit, where by definition there is no sensitivity to stabilization, to constrain the temperature dependence of $\langle\Delta E\rangle_{tot}$. No direct measurements of this property exist for C_2H_6*, although such measurements on other kinds of metastable adducts suggest mild temperature dependencies (i.e., $T^{\pm 1/2}$) can occur.[18] If for Rxn. (1) measurements were extended to lower pressures at the lower temperatures, then increased sensitivity to $\langle\Delta E\rangle_{tot}$ over the whole temperature range would result.

The second issue of the temperature dependence of the high pressure limit was first raised by Wardlaw and Marcus[11] who pointed out that a more developed dynamical model (termed Flexible Transition State Theory or FTST) of the anharmonicity of the loose degrees of freedom present at the reaction bottleneck for Rxn. (1) leads to a negative temperature dependence rather than the positive temperature dependence determined in previous models and at least one subsequent adiabatic channel model.[13] Despite differing predictions for this property, both FTST[12] and adiabatic channel theory[13] reproduce the experimental record quite well, indicating that the high pressure limit has not been constrained by the measurements over an extensive enough temperature range to determine its temperature dependence. While difficult to attain at high temperatures, measurement of the high pressure limit at depressed temperatures can be reasonably achieved at generally accessible pressures. If precise enough, such measurements could give at least the low temperature behavior of the high pressure limit.

These two issues have motivated the additional measurements on Rxn. (1) reported here. Measurements at depressed temperatures has been achieved by straight forward modifications of a technique already applied[7,8] by two of the authors (Davies and Pilling) to Rxn. (1). Measurements at low pressures have been achieved by application of the flow reactor technique.[19] In determining the absolute CH_3 concentrations in the reactor with this technique, it is necessary to account for heat and mass transfer effects because they can influence the derived bimolecular rate constants. In particular, axial and radial diffusion, viscous pressure drop and temperature rise in the reaction system, which may be caused by the energy release of the CH_3 generation and the CH_3 recombination, must be either eliminated or included in the data analysis. These effects limit the usable pressure range and the experiments reported here were therefore designed carefully in order to control and minimize them.

In addition to new measurements, this paper reports an extended comparison of the theoretical calculations of Ref. 12 to all the experimental results. In the next section, the new measurements at low pressures and moderate temperatures are described. In Section III, the measurements at lower temperatures are discussed. In Section IV, the theoretical calculations are presented. In Section V, an analytical representation of the calibrated calculations over an extended range of pressure and temperature is developed.

Measurements at Low Pressure

The discharge flow mass spectrometer apparatus used in this study has been described in detail previously[20,21] and only the main features are presented here. Teflon reactors with various diameters (12, 19, 29, and 39 mm) and approximately 55 cm length were used. The movable injector consisted of quartz glass (inner diameter 8 mm) and was coated on both sides with Teflon FEP 856-800 (Du Pont de Nemours). The heating of the flow reactors was provided by two electrical heating elements, which were wrapped around the outer surface of the reactors. The gas temperature along the reactor axis was measured directly by two teflon coated Chromel-Alumel thermocouples (Philips). One of them was positioned at the exit of the injector and the other one projected well into the reaction zone. Methyl radicals were generated by the fast reaction[22]

$$F + CH_4 \rightarrow HF + CH_3 \qquad (3)$$

The F-atoms were generated in the sidearm of the

movable injector by passing F_2 diluted in Ar through a microwave discharge (50 W, 2450 GHz). They were fed into the main carrier gas stream which contained CH_4 in large excess ($30 < [CH_4]/[F] < 150$). The methyl radicals were monitored at m/e = 15 amu with low electron energies (14 eV) to minimize interference from fragmentation of CH_4. The course of the Rxn. (1) was followed by monitoring the decay of CH_3 with time, by varying the distance between injector and detector.

The initial CH_3 concentration $[CH_3]_o$ for an experimental run is given as the CH_3 concentration at the sampling nozzle, when the injector is in its start position. $[CH_3]_o$ is always smaller than the initial F-atom concentration due to reactions in the mixing zone. Therefore a calibration procedure had to be established in order to determine absolute CH_3 concentrations. Initial CH_3 concentrations were determined by quenching the CH_3 radicals at the end of the reactor just above the sampling nozzle with the fast reaction[23]

$$CH_3 + NO_2 \rightarrow CH_3O + NO \qquad (4)$$

and measuring the NO signal at m/e = 30 amu with low electron energies (12.5 eV) in order to reduce interference from NO_2 fragmentation. This was done by injecting NO_2 in large excess ($[NO_2]/[CH_3] > 100$) through several thin teflon tubes just above the sampling nozzle. The produced NO was measured absolutely by calibration of the NO signal with a known NO flow.

Gas flows were measured and controlled by flow controllers (Tylan). The following gases (Messer-Griesheim) were used without further purification: Ar 99.999%, 5% F_2 in He 99.996%, CH_4 99.995%, NO_2 98.0%, NO 2% in He 99.996%.

Accurate determinations of $[CH_3]_o$ were critical to these experiments and the titration reaction was therefore thoroughly investigated. It could be shown by computer simulations that under the given experimental conditions the stoichiometric conversion from CH_3 to NO was not disturbed by subsequent reactions. This was also confirmed by an experimental investigation of the titration reaction. Calibration curves were measured for each set of CH_3 decay profiles. They were obtained by measuring the NO signal as a function of the decrease in the CH_3 signal upon addition of NO_2 and were used to calibrate the respective CH_3 signals. The calibration procedure will be discussed in more detail in a forthcoming publication.[24]

Under experimental conditions where diffusion effects can be neglected, the usual second order plots ($1/[CH_3]$ versus time) yielded straight lines indicating that the CH_3 wall loss was negligibly small, in accord with earlier work.[8] Bimolecular rate constants could be extracted from the slope of these straight lines in the usual way. In the presence of diffusion, however, the evaluation procedure must be modified. Since diffusion is pronounced for high $[CH_3]$, its effect imposes some curvature to the $1/[CH_3](t)$ graphs at early times. In this case the slopes of the tangents of the $1/[CH_3](t)$ curves are concentration dependent. It can be shown that the subtangents of these tangents represent first order rate constants (K_I). For the correction of diffusion effects, the well known correction formula[25a] cannot be applied since it refers to pseudo first order reactions. The present case, a second order reaction in a diffusive flow was treated by solving the appropriate differential equation. For the one dimensional case (e.g. low pressures) this led to the correction formula[25b]

$$K_{I,corr} = K_I(1 + K_I D/v^2 - D/vK_I \cdot dK_I/dz) \qquad (5)$$

where K_I denotes the first order rate constant, v the linear flow velocity, D the diffusion coefficient for CH_3 in argon, and dK_I/dz the limiting slope of K_I with respect to the distance z equal to vt. In the absence of wall effects, the third term in the brackets approximately equals the negative of the second one. Therefore, this formula means that, for a purely second order reaction, the diffusion correction has to be doubled. For higher pressures, $[CH_3]$ is also a function of the radius. This is implicitly accounted for by using an effective diffusion coefficient[25a] instead of D which is given as

$$D_{eff} = D + r^2v^2/48D \qquad (6)$$

where r denotes the reactor radius. Values of D were calculated for the pressures and temperatures used in this study according to the method of Hirschfelder et al..[26] It can be seen from equation (5) that the diffusion correction can be minimized by choosing the appropriate reactor radius and the appropriate flow velocity. The diffusion corrections applied were always small (4–30%) and could be neglected in most experiments of this study.

The viscous pressure drop Δp was measured in extra experimental runs by connecting a capacitance manometer (MKS Baratron) to the movable injector. When Δp could not be neglected, corrections (2–12%) were made as described in the literature.[25] The reaction induced temperature rise was measured in all experiments by the two thermocouples in the injector. Even at the lowest pressures, the temperature rise was <4 K and could therefore be neglected in the data evaluation. However, at 408 K, the electrical heating elements could not provide an entirely flat temperature over the whole reaction length in the flow tube. A temperature gradient ($\Delta T < 30$ K) prevailed within the first 3 cm of about 33 cm total reaction length in the flow tube. A small correction (10%) was there-

fore applied to the respective rate constants according to a method outlined previously.[27]

At 300 K and 408 K, at least 5 measurements were performed for each value of [M] by varying the initial CH_3 concentrations. The measured values of k_1 are estimated to be accurate to ±20%. This includes the estimated uncertainties in the measured experimental parameters (T,[M], $[CH_3]_o$ and k_1). The conditions of all experiments and the results obtained are given in Table I and two of the panels of Fig. 1. As shown in Fig. 1, where overlap with previous measurements[8] is possible (only at 300 K), satisfactory agreement is found. However, these new low pressure results do show more substantial fall off than would have been extrapolated from previous measurements via the theoretical calculations of Ref. 12.

Measurements at Low Temperature

The basis of the experimental work has previously been described[7,8,28] Methyl radicals were generated from acetone at 193 nm using a Lumonics TE861S-4 excimer laser. Acetone is a very clean source of CH_3, with more than 95% of the photolysis proceeding via the channel leading to $2CH_3$ + CO.[29] CH_3 was monitored via its UV absorption band at 216.36 nm, using a 450 W xenon lamp as the background source and dispersing the radiation with a Hilger Monospek 1000 monochromator with a bandpass of 0.6 nm.

The reaction vessel was a 2 cm diameter specrosil tube of length 50 cm. with specrosil end windows. It was contained in a carbon dioxide/acetone bath which maintained the temperature at 200 ± 3 K. The laser radiation was expanded via a telescope to produce a parallel beam which overfilled the cell. The beam was deflected along the axis of the cell using a dichroic mirror reflecting at 193 nm, but transmitting at 216 nm. Light from the xenon lamp was passed through the dichroic along the same axis. A 2 cm filter solution of 0.01M NaCl was placed in front of the monochromator slit to remove the laser radiation without affecting the monitoring beam.

The methods of data analysis have been described previously.[7,8,28] The radical decays exclusively by recombination and the experiment returns values of k_1/σ, where σ is the CH_3 absorption cross-section. Absolute values of σ are required to determine k_1 and σ is temperature dependent. Its determination has previously been described, when the experimental values were also compared with simulations of the temperature dependence. Excel-

TABLE I
Conditions and results for experimental measurements

T/K	p/m bar	10^{16}[Ar] (molecules/cm^3)	$10^{12}[CH_3]_o$ (molecules/cm^3)	$10^{11}k_1$ (cm^3/molec-sec)
200[a]	12.6	41.5	(b)	6.65
	33.4	123.	(b)	6.61
	65.7	241.	(b)	7.11
	98.4	361.	(b)	6.80
	131.	479.	(b)	6.86
	197.	724.	(b)	6.66
	262.	961.	(b)	6.87
	393.	1440.	(b)	6.90
	528.	1940.	(b)	7.30
300[c]	0.195	0.47	2.17–5.06	1.7
	0.59	1.42	1.97–4.01	2.6
	1.00	2.40	1.56–5.24	3.3
	1.99	4.80	2.32–4.10	4.0
	2.88	6.95	1.81–5.30	4.1
408[c]	0.39	0.69	2.29–5.07	1.1
	1.08	1.93	2.07–5.05	1.7
	2.08	3.69	3.14–4.73	2.1
	4.20	7.46	2.25–4.41	2.9

[a]Laser flash photolysis results.
[b]$[CH_3]_o$ was varied over the range 10^{13}–10^{14}.
[c]Flow reactor results.

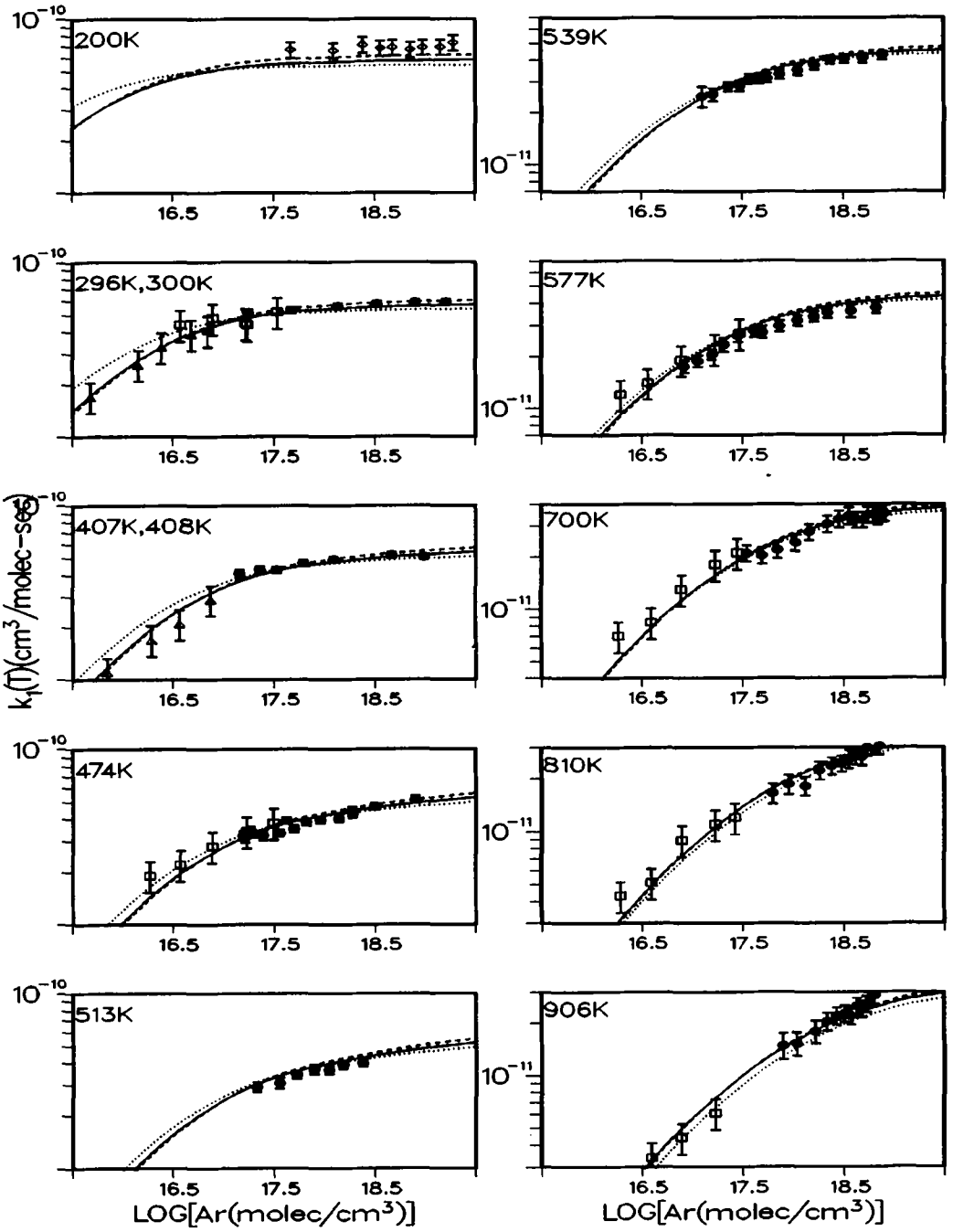

FIG. 1. Comparison of measured (triangle, diamond: Table I; square, circle: Ref. 8) and calculated rate constants k_1 versus Ar buffer gas concentration at ten different temperatures. The three calculations are (. . .) α = .65 Å^{-1}, $\langle\Delta E\rangle_{tot}$ = −186 cm^{-1}; (—) α = .73 Å^{-1}, $\langle\Delta E\rangle_{tot}$ = −76 (T/296 K)$^{1.0}$; (---) α = .81 Å^{-1}, $\langle\Delta E\rangle_{tot}$ = −64 (T/296 K)$^{1.1}$.

lent agreement was obtained and simulations[30] have been employed in the present study to extend the absolute values of σ down to 200 K. Over the temperature range 150–298 K, the absorption cross-section is best expressed by: $\sigma = \{5.78 - 5.48\} \times 10^{-3}(T/K) \times 10^{17}$ cm^2-molecule^{-1}, with an estimated uncertainty (two standard deviations) of ± 5%.

The final measured values of k_1 at 200 K are listed in Table I and displayed in the top panel of Fig. 1.

Theory

The new measurements reported in Table I augment the experimental data set that is available for comparison to theory. Accordingly, the theoretical calculations presented in Ref. 12 will here be extended to a comparison of the new data. A brief review of the theoretical model is in order (details can be found in Refs. 11 and 12). The model consists of a parameterized potential energy surface on which the dynamics is calculated via a weak-coupling corrected variational activated complex RRKM calculation based on a FTST description of the transition state. The model has two parameters. The first is α which controls the presumed exponential switching of structures and conserved frequencies along the reaction path connecting CH_3 reactants to C_2H_6 product. The remaining parts of the potential are empirically derived and include a highly anharmonic treatment of the transitional frequencies of C_2H_6 that evolve along the reaction path from the free rotations of the reactants. The second parameter is $\langle\Delta E\rangle_{tot}$ which assumes the form:

$$\langle\Delta E\rangle_{tot} = \langle\Delta E\rangle_{tot}(296\text{ K})(T/296\text{ K})^n \qquad (7)$$

where $\langle\Delta E\rangle_{tot}(296\text{ K})$ and n are adjustable.

In the work reported here, both adjustable parameters α and $\langle\Delta E\rangle_{tot}$ are optimized to achieve the best agreement with the data presented in the previous sections and the data originally used in Ref. 12. "Best agreement" was determined by the minimization of the average error defined to be, as in Ref. 12, the root means square (rms) of the rms relative error between theory and experiment for each set of measurements made by a specific technique at a given temperature. Therefore, in this study, the average error will be constructed from the relative errors for the 15 original sets of measurements[8,12] augmented by the relative errors for the three sets of measurements in Table I.

The results of the optimization of the parameters is displayed in Fig. 1 for the 10 different temperatures from 200 K to 906 K surveyed by all the measurements. Three different kinds of optimizations are reported. One constrains $\langle\Delta E\rangle_{tot}$ be independent of temperature, i.e., n = 0.0. The resulting parameter values are $\alpha = .65$ Å^{-1} and $\langle\Delta E\rangle_{tot} = -186$ cm^{-1}. The second is an unconstrained optimization resulting in parameter values of $\alpha = .73$ Å^{-1} and $\langle\Delta E\rangle_{tot} = -76\ (T/296\text{ K})^{1.0}$ cm^{-1}. The third constrains α to be .81 Å^{-1} resulting in an optimized value for $\langle\Delta E\rangle_{tot}$ of $-64\ (T/296\text{ K})^{1.1}$.

The main conclusion from Fig. 1 is that the presence or absence of temperature dependence in $\langle\Delta E\rangle_{tot}$ can be distinguished by the measurements. This can be seen by considering only the first two calculations. Without the temperature dependence in $\langle\Delta E\rangle_{tot}$, the first calculation has an average error of 13.5% and falls noticeably above the low pressure measurements reported here for 300 K and 408 K. With the temperature dependence in $\langle\Delta E\rangle_{tot}$, the second calculation has an average error of 10.5% and substantial agreement with these two low pressure measurement sets. In Ref. 10, the original data set could not distinguish these two kinds of models. In that work, the final theoretical representation selected was a temperature independent value of $\langle\Delta E\rangle_{tot}$ of -205 cm^{-1} for $\alpha = .70$ with an average error of 9.9%. Thus the three additional data sets described in the previous sections has increased the average error by about 0.6%, a rather minor amount.

A second conclusion that can be drawn from Fig. 1 is that optimization of α produces rate constants that fall below the approximately 10% error bars associated with the new measurements at 200 K. This is the only outstanding systematic deviation over the ten temperatures surveyed in the figure for the second and fully optimized calculation. Because of the approach to the high pressure limit at this low temperature, the $\langle\Delta E\rangle_{tot}$ parameter values have a very minor effect on the agreement between theory and experiment. Only changing the value of α can improve the agreement. The third calculation shown in Fig. 2 represents the minimization of the temperature dependent $\langle\Delta E\rangle_{tot}$ parameters under the restriction that alpha = .81 Å^{-1}, the lowest value of α for which the calculated rate constant falls within the measured error bars at 200 K. This restricted optimization has an average error of 10.7%, only 0.2% higher than the fully optimized result. While agreement at 200 K has been noticeably improved, the higher pressure results at 513 K, 539 K and 577 K tend to be systematically a little high.

In Fig. 2, the calculated high pressure limit of k_1 is displayed for all three calculations in Fig. 2 along with the one directly measured value[6] at room temperature and the average of the 200 K measured values (with $\pm 2\sigma$ error bars). This average approximately represents the measured high pressure limit at 200 K as the data displays little pressure dependence (see Fig. 2) and at lower temperatures the limit should be reached at lower

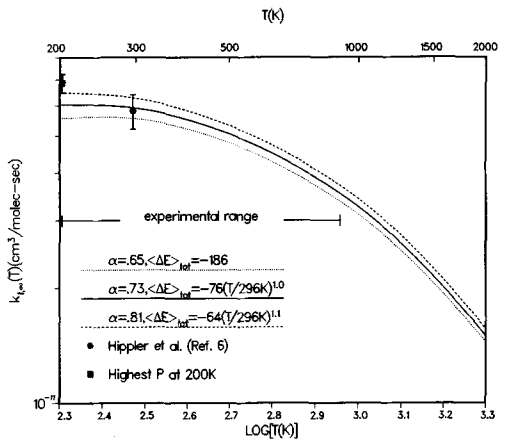

FIG. 2. Comparison of measured and calculated high pressure limiting rate constants $k_{1,\infty}$ versus log(T). See text for details.

pressures. The figure indicates that all three calculations fall within the error bars of the room temperature measurement. Only the calculation constrained to $\alpha = .81$ Å^{-1} falls within the error bars at 200 K but the other calculations are close. For all three calculations there is substantial negative temperature dependence, as in other FTST calculations[12,14] of this quantity. The experimental results in the figure tend to support a negative temperature dependence.

The optimized temperature independent value of $\langle\Delta E\rangle_{tot}$ of -186 cm^{-1} is quite consistent with measured values on other systems.[12] However, the optimized temperature dependent value of $\langle\Delta E\rangle_{tot}$ shows an approximately linear dependence on temperature. Deviations of ± 0.4 about a unit power to the temperature dependence were found not to substantially degrade agreement with experiment. This degree of temperature dependence is noticeably larger than direct measurements[18] of this property on other systems. However, the 700 K range covered by this indirect study is approximately double that of the direct work and is the broadest temperature range for which the temperature dependence of $\langle\Delta E\rangle_{tot}$ has ever been studied.

Of the three calculations in Figs. 1 and 2, the constrained calculation with α set to .81 Å^{-1} is considered the best supported by experiment. Although this calculation does not fully minimize the average error, it does minimize errors in a way most consistent with the varying error bars of the measurements to produce the representation most free of systematic error. Accordingly this calculation will be used in the next section to produce an analytic fit.

Analytic Representation of $k_1(T,[M])$

With the variable parameters in the model optimized by the experimental data, the RRKM calculations can be used to optimize an analytic fitting function. Analytic forms are particularly valuable for incorporation in numerical models of complex kinetic systems. The RRKM calculations to be fit are designed to represent the rate constant from 200 K to 2000 K at pressures where the rate is at least 10^{-12} cm^3/molecule-sec. The work in Ref. 12 differs slightly from that here in that the previous effort included at 200 K only the rate constants near the high pressure limit in the fit.

The functional form contains 11 parameters and is described in detail in Ref. 12. The best fit found is

$$k_{LP} = 0.313 \times 10^{-11}\, T^{-5.246}\, e^{-858/T}$$
$$F_{cent} = 0.595\, e^{-T/1120} + 0.405\, e^{-T/69.6}$$
$$k_{HP} = 0.153 \times 10^{-6}\, T^{-1.174}\, e^{-320/T} \qquad (8)$$

This fit has an rms error to the calculated data set of 7.1% with no error greater than 18.2%. The rms error with the original experimental values is 10.9%. This is comparable to the analytic representation achieved in Ref. 12.

There are two caveats to the above representation. First, in the original nature of these forms, the HP and LP subscripts stand for the high and lower pressure limit. However, in this fit, they should be regarded *only* as fitting functions to represent over the given temperature range at all pressures where the rate constant is greater than 10^{-12} cm^3/molecule-sec. In particular, the k_{LP} bears little resemblance to the true low pressure limit and the k_{HP} is not an exact fit to the high pressure limit results in Fig. 2. Second, at the higher temperatures covered by this fit, disproportionation channels are accessible, making the analytic expression underestimate the *total* rate of loss of CH_3. In Ref. 15, a less quantitative but similar fit without these caveats is discussed.

Acknowledgment

This research was supported in part by the Office of Basic Energy Sciences, Division of Chemical Sciences, U.S. Department of Energy under contract W-31-109-Eng-38.

REFERENCES

1. WARNATZ, J.: Combustion Chemistry (Gardiner, W. C., Ed.), Chap. 5, Springer-Verlag, 1984.
2. KERR, J. A., AND MOSS, S. J.: CRC Handbook

of Bimolecular and Termolecular Gas Reaction, CRC Press, 1981.
3. BAULCH, D. L., DUXBURY, J.: Comb. Flame 37, 313 (1980).
4. SKINNER, G. B., ROGERS, D., PATEL, K. B.: Int. J. Chem. Kinet. 13, 481 (1981).
5. GLANZER, K., QUACK, M., TROE, J.: J. Chem. Phys. Lett. 39, 304 (1976).
6. HIPPLER, H., LUTHER, K., RAVISHANKARA, A. R., TROE, J.: Z. Phys. Chem. Neue Folge 142, 1 (1984).
7. MACPHERSON, J. T., PILLING, M. J., SMITH, M. J. C.: Chem. Phys. Lett. 94, 430 (1983); MACPHERSON, J. T., PILLING, M. J., SMITH, M. J. C.: J. Phys. Chem. 89, 2268 (1985).
8. SLAGLE, I. R.; GUTMAN, D., DAVIES, J. W., PILLING, M. J.: J. Phys. Chem. 92, 2455 (1988).
9. WAAGE, E. V., RABINOVITCH, B. S.: Int. J. Chem. Kinet. 3, 105 (1971).
10. HASE, W. L.: J. Chem. Phys. 64, 2442 (1976).
11. WARDLAW, D. M., MARCUS, R. A.: J. Phys. Chem. 90, 5383 (1986).
12. WAGNER, A. F., WARDLAW, D. M.: J. Phys. Chem. 92, 2462 (1988).
13. TROE, J. Twenty-Second Symposium (International) on Combustion, p. 843, The Combustion Institute, 1989; QUACK, M., TROE, J.: Ber. Bunsen-Ges. Phys. Chem. 78, 240 (1974).
14. DARVESH, K. V., BOYD, R. J., PACEY, P. D.: J. Phys. Chem. 93, 4772 (1989).
15. STEWART, P. H., LARSON, C. W., GOLDEN, D. M.: Combustion and Flame 75, 25 (1989).
16. TROE, J.: J. Chem. Phys. 66, 4745 (1977).
17. TROE, J.: J. Phys. Chem. 83, 114 (1979).
18. HEYMANN, M., HIPPLER, H., TROE, J.: J. Chem. Phys. 80, 1853 (1984).
19. HOWARD, C. J.: J. Phys. Chem. 83, 3 (1979).
20. GROTHEER, H. H., RIEKERT, G., WALTER, D., JUST, TH.: Chem. Phys. Lett. 148, 530 (1988).
21. GROTHEER, H. H., RIEKERT, G., WALTER, D., JUST, TH.: J. Phys. Chem. 92, 4028, (1988).
22. BAULCH, D. L., COX, R. A., CRUTZEN, P. J., HAMPSON, R. F. JR., KERR, J. A., TROE, J., WATSON, R. T.: J. Phys. Chem. Ref. Data 11, 334, (1982).
23. YAMADA, F., SLAGLE, I. R., GUTMAN, D.: Chem. Phys. Lett. 83, 409 (1981).
24. WALTER, D., GROTHEER, H. H., JUST, TH.: to be published.
25. (a) KEYSER, L. F.: J. Phys. Chem. 88, 4750 (1984); (b) GROTHEER, O., DAMM, R., GROTHEER, H. H.: (to be published).
26. HIRSCHFELDER, J. O., CURTISS, C. F., BIRD, R. B.: Molecular Theory of Gases and Liquids, New York 1954.
27. MEIER, U., GROTHEER, H. H., RIEKERT, G., JUST, TH.: Chem. Phys. Lett. 133, 162 (1987).
28. TULLOCH, J. M., MACPHERSON, M. T., MORGAN, C. A., PILLING, M. J.: J. Phys. Chem. 86, 3812 (1982).
29. LIGHTFOOT, P. D., KIRWAN, S. P., PILLING, M. J.: J. Phys. Chem. 92, 4938 (1988).
30. ASHFOLD, M. N. R.: private communication.